

# Generalized Tolman-Oppenheimer-Volkoff model and neutron stars

A. Rahmansyah<sup>1</sup>, D. Purnamasari<sup>1</sup>, R. Kurniadi<sup>2</sup>, and A. Sulaksono<sup>1,\*</sup>

<sup>1</sup>*Departemen Fisika, FMIPA, Universitas Indonesia, Depok 16424, Indonesia*

<sup>2</sup>*Departemen Fisika, FMIPA, Institut Teknologi Bandung, Jl. Ganesha 10, Bandung 40132, Indonesia*



(Received 24 June 2022; accepted 27 September 2022; published 21 October 2022)

This work is motivated by the existence of mapping the extended theory of gravity with a standard energy-momentum tensor to general relativity with a modified energy-momentum tensor. We construct a modified anisotropic energy-momentum tensor from a standard isotropic energy-momentum tensor by adding a “geometrical correction” to precisely reproduce the Tolman-Oppenheimer-Volkoff equations predicted by the generalized Tolman-Oppenheimer-Volkoff (GTOV) model. This construction aims to calculate the moment of inertia ( $I$ ) and tidal deformability ( $\Lambda$ ) of neutron stars (NSs) within the GTOV model. Therefore, we can comprehensively investigate the role of each free parameter of the GTOV model in NS properties. Furthermore, through this construction we can also utilize physically acceptable stability conditions for anisotropic stars to constrain the physical range of each parameter value and investigate the existence of a correlation among the parameters of the GTOV model. Except for  $\alpha$ , we find that the values of the GTOV free parameters can be limited to acceptable ranges. We also find that the parameters  $\theta$ ,  $\chi$ , and  $\beta$  are correlated, and the parameter  $\Gamma \rightarrow 0$ . With these free parameter ranges in hand, we study the role of each parameter of the GTOV model in NS properties, including  $I$  and  $\Lambda$ . We also revisit the hyperon puzzle in NSs within the GTOV model. We find that the  $\theta$  parameter plays a crucial role in controlling the NS maximum mass value. We also find that the threshold  $k_2$  peak for NS is  $k_2 \approx 0.167$ . Furthermore, if we use parameter sets with  $\theta = -1$ , the mass-radius predictions are compatible with recent NICER data on PSR J0030 + 0451 and PSR J0740 + 6620.

DOI: [10.1103/PhysRevD.106.084042](https://doi.org/10.1103/PhysRevD.106.084042)

## I. INTRODUCTION

Neutron stars (NSs) have a relatively large compactness (i.e.,  $C \lesssim \frac{1}{3}$ ) and high densities (i.e., around several times the nuclear saturation density  $\rho \approx 3 \times 10^4 \frac{\text{g}}{\text{cm}^3}$ ). Therefore, observational data of neutron star’s properties are crucial to investigate the equation of state (EOS) of nuclear matter at high densities and to probe the impact of gravity within both general relativity (GR) [1–3] and extended theories of gravity (ETGs) [4–6]. We can extract the NS mass ( $M$ ), radius ( $R$ ), inertia moment ( $I$ ), and tidal deformability ( $\Lambda$ ) from astronomical observations. For example, observations by the Neutron Star Interior Composition Explorer (NICER) can simultaneously constrain the  $M$ ,  $R$ , and  $I$  of PSR J0030 + 0451 [7,8] and PSR J0740 + 6620 [9,10]. We can also obtain information on the merger of binary NSs from gravitational waves (GWs). The GW events GW170817 [11–13] and GW190425 [14] and their electromagnetic counterparts [15,16] can provide relatively accurate  $\Lambda$  and  $M$  values, as well as other properties of NSs. We need to note that sets of observational results from different systems can also be used to constrain a shared underlying NS property through a hierarchical inference scheme.

For a recent report on this scheme, please see Ref. [17] and references therein. Furthermore, testing gravity using NSs is challenging since the EOS and the gravity theory to describe NSs are uncertain. One possible way to overcome this issue is by employing the EOS-independent (universal) relation between  $I$ ,  $L$ , and  $Q$ , where  $L$  is the tidal Love number and  $Q$  is the quadrupole moment of NSs. See Ref. [6] for a recent report on scalar-Gauss-Bonnet gravity theory, and the references therein for the GR and other ETG cases. Information on  $M$ ,  $R$ ,  $I$ ,  $\Lambda$  or  $L$ , and  $Q$  are essential to understanding the EOS and composition of NSs.

References [18–21] reported that one can map the Einstein field equations of ETGs using a standard isotropic energy-momentum tensor for describing matter into the one of Einstein field equation of GR theory but by using the apparent or modified energy-momentum tensor; see the detailed discussions in Refs. [18–21] and references therein. Wojnar and Velten [19] also demonstrated that the modified Einstein field equations of a large class of ETGs can be written generally into GR Einstein’s field equations with an effective energy-momentum tensor. The energy-momentum tensor consists of energy-momentum tensor of actual EOS of matter and energy-momentum tensor from geometrical source. The explicit form of this energy-momentum tensor correction depends on the specific ETG used, and the

\*anto.sulaksono@sci.ui.ac.id

pressure of NSs might be anisotropic due to this term [19] [e.g., the Eddington-inspired Born-Infeld (EiBI) case]. In the EiBI case, the pressure in the apparent EOS becomes anisotropic even though the pressure in the actual EOS of the matter is isotropic [18].

A few years ago, Mota *et al.* [22] introduced a free *ad hoc* parametrization of the Tolman-Oppenheimer-Volkoff (TOV) model to overcome the hyperon puzzle in NSs. The model is known as the generalized TOV (GTOV) model. From a phenomenological point of view, this model is attractive because adding more free parameters to every term of the TOV equations makes the model more flexible if we compare this model's predictions for  $M$  and  $R$  with observational data. This model extends the previous proposal known as the free parametrized TOV (PTOV) model [23]. The PTOV model aims to investigate the correspondence between each TOV term with possible terms in ETG and to distinguish the role of ETG term using NS properties. However, we have difficulty calculating other observable properties of NSs— $I$ ,  $\Lambda$  or  $L$ , and  $Q$ —and examining the stability of stars in the relative extreme values of the free parameter due to this model does not provide TOV equations from Einstein's field equations.

Inspired by the possibility of mapping ETG with standard matter into GR with modified matter, we construct a modified anisotropic energy-momentum tensor to obtain the TOV equations of GTOV or PTOV models. Using the Einstein field equations with both a standard, slowly rotating metric and a tidal deformation metric, the  $I$  and  $\Lambda$  of NSs can be calculated. Furthermore, we employ physically acceptable stability conditions for an anisotropic object [24–26] to constrain the GTOV model's parameters and study the correlations among the parameters. We hope that we can reduce the number of free parameters into physically parameters. With these free-parameter ranges in hand, we revisit the hyperon puzzle in NSs to test whether the GTOV model can resolve this issue.

The paper is organized as follows. In Sec. II we briefly discuss the anisotropic energy-momentum tensor correction in GR that can reproduce the TOV equations of the GTOV model. We also show the explicit expressions to calculate the mass-radius relation, moment of inertia, and tidal deformability for the GTOV model. In Sec. III we use stability conditions for anisotropic objects to reduce the number of free parameters of the GTOV model. In Sec. IV we discuss the structure of EOSs and the composition of NSs by taking into account hyperons in EOSs. In Sec. V we discuss the numerical results. Finally, we give our conclusions in Sec. VI.

## II. GENERALIZED TOV EQUATIONS AND EFFECTIVE ENERGY-MOMENTUM TENSOR

In this section we construct an effective energy-momentum tensor with an effective energy density and anisotropic pressure. If we define the specific form of the effective energy density and the difference between radial

and tangential pressure forms, the corresponding TOV equations of this model can be recast exactly into the TOV equations of the GTOV model. In this way, we can calculate all NS properties, including  $I$  and  $\Lambda$ . The effective energy-momentum tensor is defined as [1]

$$\bar{T}_{\mu\nu} \equiv \bar{\epsilon}u_\mu u_\nu + Pk_\mu k_\nu + Q[g_{\mu\nu} + u_\mu u_\nu - k_\mu k_\nu], \quad (1)$$

where  $\bar{\epsilon}$  is the effective energy density which consists of the actual energy density of matter and the correction term from the geometry.  $P$  is the radial pressure,  $Q$  is the tangential pressure,  $u_\mu$  is the fluid 4-velocity,  $k_\mu$  is the unit radial vector orthogonal to  $u_\mu$ , and  $g_{\mu\nu}$  is the spacetime metric. The spacetime metric is given by

$$g_{\mu\nu} = \text{diag}[e^\nu, -e^\lambda, -r^2, -r^2 \sin^2 \theta], \quad (2)$$

where  $\nu = \nu(r)$  and  $\lambda = \lambda(r)$ . From the Einstein field equations, we obtain the following three relations:

$$e^{-\lambda} \left[ \frac{\lambda'}{r} - \frac{1}{r^2} \right] + \frac{1}{r^2} = 8\pi G \bar{\epsilon}, \quad (3)$$

$$e^{-\lambda} \left[ \frac{\nu'}{r} + \frac{1}{r^2} \right] - \frac{1}{r^2} = 8\pi G P, \quad (4)$$

$$e^{-\lambda} \left[ \frac{\nu''}{2} + \frac{(\nu')^2}{4} - \frac{\nu'\lambda'}{4} + \frac{\nu'}{2r} - \frac{\lambda'}{2r} \right] = 8\pi G Q. \quad (5)$$

By manipulating Eqs. (3), (4), and (5), we obtain the following TOV equations:

$$\frac{dP}{dr} = -\frac{G(\bar{\epsilon} + P)(M + 4\pi r^3 P)}{r(r - 2GM)} - \frac{2\sigma}{r}, \quad (6)$$

and

$$\frac{dM}{dr} = 4\pi \bar{\epsilon} r^2, \quad (7)$$

where  $\sigma \equiv P - Q$  [1].

We define the particular form of  $\bar{\epsilon}$  and  $\sigma$  in Eqs. (6) and (7) as

$$\bar{\epsilon} \equiv \tilde{\epsilon} + \bar{\Gamma}, \quad (8)$$

and

$$\sigma \equiv \frac{r}{2} \tilde{\Gamma} + \frac{G(\tilde{\epsilon} + P)(M + 4\pi r^3 P)}{2(r - 2GM)} \Delta. \quad (9)$$

Note that in Eqs. (8) and (9),  $\tilde{\epsilon}$ ,  $\bar{\Gamma}$ ,  $\tilde{\Gamma}$ , and  $\Delta$  are defined as

$$\tilde{\epsilon} \equiv \epsilon + \theta P, \quad (10)$$

$$\bar{\Gamma} \equiv \frac{\Gamma\sqrt{\epsilon}M}{4\pi r^2}, \quad (11)$$

$$\bar{\Gamma} \equiv -\frac{G\bar{\Gamma}(M + 4\pi r^3 P)}{r(r - 2GM)}, \quad (12)$$

and

$$\Delta \equiv \bar{\alpha}(1 + \bar{\beta})(1 + \bar{\chi}) - 1. \quad (13)$$

As we can see in Eq. (13), the  $\Delta$  term depends on three functions, i.e.,  $\bar{\alpha}$ ,  $\bar{\beta}$ , and  $\bar{\chi}$ , which depend on the GTOV parameters. The explicit forms of these functions are

$$\bar{\alpha} = \alpha + 1, \quad (14)$$

$$\bar{\beta} = \frac{P(\beta - \theta - 1)}{\tilde{\epsilon} + P}, \quad (15)$$

and

$$\bar{\chi} = \frac{4\pi r^3 P(\chi - 1)}{M + 4\pi r^3 P}. \quad (16)$$

If we substitute all of these terms into standard the TOV equations with an anisotropic pressure [i.e., Eqs. (6) and (7)], after a little bit of algebra we can obtain exactly the GTOV equations [22], i.e.,

$$\frac{dP}{dr} = -\frac{G(1 + \alpha)(\epsilon + \beta P)(M + 4\chi\pi r^3 P)}{r(r - 2GM)}, \quad (17)$$

and

$$\frac{dM}{dr} = 4\pi r^2(\epsilon + \theta P) + \Gamma\sqrt{\epsilon}M, \quad (18)$$

where  $\alpha$ ,  $\beta$ ,  $\chi$ ,  $\theta$ , and  $\Gamma$  are free parameters of the GTOV model. This means that Eqs. (8) and (9) play a role in mapping from anisotropic GR to the GTOV model. Furthermore, we can calculate an NS's tidal deformability and moment of inertia using this GR framework.

Except for  $\Gamma$ , the physical meaning of these parameters was discussed in Ref. [23]. Then, Ref. [22] introduced the  $\Gamma$  parameter because the author wanted to analyze the possible new effects that might arise from  $dM/dr$  equation. It is worth noting that  $\alpha$  parametrizes the deviation of the gravitational coupling value, i.e.,  $G_{\text{eff}} = G(1 + \alpha)$ , where  $G$  is the gravitational coupling [22,23]. Some modified gravity theories predict  $\alpha$  whose form can be seen clearly in their nonrelativistic limit expression. For instance,  $f(R)$  theory in Refs. [22,23,27]. Note that  $\beta$ ,  $\chi$ , and  $\theta$  affect the pressure contribution of the TOV equations, i.e., they relate inertial pressure, self-gravity, and gravitational mass of stellar dense objects, respectively. Furthermore, the term relates to  $\chi$  is genuine GR [22,23]. In a recent report, the NS

mass was shown to be relatively sensitive to variations in the value of  $\chi$  [28]. On the contrary, the radius is not too sensitive to variations in the value of  $\chi$ . In GR, the value of each parameter is  $\alpha = 0$ ,  $\beta = 1$ ,  $\chi = 1$ ,  $\theta = 0$ , and  $\Gamma = 0$ . The deviation from these GR values indicates the existence of modified gravity. As far as we know, the reported observational constraints are only for  $\alpha$  and  $\chi$  [29,30]. The best-fit range for  $\alpha$  extracted from observations is  $0.04 \lesssim \alpha \lesssim 0.15$  [29]. However, the big bang nucleosynthesis (BBN) fitting results for  $\chi$  are  $\chi = 1.0 \pm 0.14$  and  $\chi = 0.84 \pm 0.25$ , and the data are strongly incompatible with  $\chi = 0$ . The corresponding fitting results only slightly depend on the details of the observable involved. This means that BBN data is consistent with the value predicted by GR; see Ref. [30] and references therein for a detailed discussion of the  $\chi$  constraint from BBN. It is also worth noting that one of the ETGs, i.e., energy-momentum squared gravity (T-squared gravity) theory, has a relatively similar TOV equation structure as those of the GTOV model; see Ref. [31] and references therein for detailed applications of the T-squared gravity model. The TOV equations of this model with the coupling of energy-momentum squared gravity  $\kappa$  are [31]

$$\frac{dP}{dr} = -\frac{G[1 + \alpha(\epsilon, P)](\epsilon + \beta P)[M + \chi(\epsilon, P)4\pi r^3 P]}{r(r - 2GM)}, \quad (19)$$

with

$$\chi(\epsilon, P) = 1 + \kappa \frac{\epsilon^2}{P} \left(1 + \frac{3P^2}{\epsilon^2}\right),$$

$$\alpha(\epsilon, P) = 2\kappa\epsilon \left(1 - \frac{\partial\epsilon}{\partial P}\right),$$

and

$$\frac{dM}{dr} = 4\pi r^2[\epsilon + \theta(\epsilon, P)P + \kappa\epsilon^2], \quad (20)$$

where  $\theta = \kappa(8\epsilon + 3P)$ . The fact that  $\alpha$ ,  $\chi$ , and  $\theta$  in T-squared gravity theory depend on the free parameters  $\kappa$ ,  $P$ , and  $\epsilon$ , the main difference appears in the term couple by  $\Gamma$  in GTOV model is  $\sqrt{\epsilon}M$  while the  $\kappa$ -term of T-squared gravity theory is in the form of  $\epsilon^2$ . We will discuss the role of these parameters in more detail for a stellar configuration later.

The dimensionless tidal deformability can be expressed as [32]

$$\Lambda = \frac{2k_2}{3C^5}, \quad (21)$$

where  $k_2$  and  $C$  are the electric-tidal Love number and NS compactness, respectively. The NS compactness can be expressed as

$$C = \frac{2GM}{R}, \quad (22)$$

where  $M$  and  $R$  are the NS mass and radius, respectively. We have to solve a first-order differential equation to obtain  $k_2$  [1],

$$r \frac{dy}{dr} + y^2 + B_1 y + B_2 r^2 = 0, \quad (23)$$

where

$$B_1 = \frac{r - 4\pi r^3(\bar{\epsilon} - P)}{r - 2GM}, \quad (24)$$

$$B_2 = \frac{4\pi r \left( 4\epsilon + 8P + \frac{(\bar{\epsilon} + P) \left( 1 + \frac{d\epsilon}{dP} \right)}{1 - \frac{d\sigma}{dP}} + 4\sigma \right)}{r - 2M} - 4 \left( \frac{M + 4\pi r^3 P}{r^2 \left( 1 - \frac{2GM}{r} \right)} \right)^2. \quad (25)$$

More details about obtaining Eq. (23) can be found in Ref. [1]. Here, we set the initial value of  $y$ , i.e.,  $y(0) = 2$ , to solve Eq. (23). Moreover, we solve it simultaneously with the anisotropic TOV equations. After solving it, we can compute the  $k_2$  value,

$$k_2 = \frac{B_3}{B_4}, \quad (26)$$

where

$$B_3 = \frac{8}{5}(1 - 2C)^2 C^5 (2C(Y - 1) - Y + 2), \quad (27)$$

$$B_4 = 2C(4(Y + 1)C^4 + (6Y - 4)C^3) + 2C((26 - 22Y)C^2 + 3(5Y - 8)C - 3Y + 6) - 3(1 - 2C)^2(2C(Y - 1) - Y + 2) \ln \left( \frac{1}{1 - 2C} \right), \quad (28)$$

where  $Y = y(R)$ . Therefore, we can compute the dimensionless tidal deformability after we obtain  $k_2$  and  $C$ .

To obtain the moment of inertia, we have to solve two first-order differential equations,

$$\frac{d\tilde{\omega}}{dr} = \frac{6}{r^4} e^\nu \left( 1 - \frac{2GM}{r} \right)^{-1/2} \tilde{\kappa}$$

$$\frac{d\tilde{\kappa}}{dr} = \frac{8\pi}{3} \frac{r^4 e^{-\nu} (\bar{\epsilon} + P)}{\left( 1 - \frac{2GM}{r} \right)^{1/2}} \left( 1 + \frac{\sigma}{\bar{\epsilon} + P} \right) \tilde{\omega}. \quad (29)$$

More details about obtaining Eq. (29) can be found in Ref. [1]. Here, we use the slowly rotating approximation. We solve two first-order differential equations using the Runge-Kutta methods with boundary conditions:

$$\tilde{\omega}(R) = 1 - \frac{2I}{R^3},$$

$$\tilde{\kappa}(R) = I, \quad (30)$$

where  $I$  is the moment of inertia of NSs.

### III. ANALYSIS OF GENERALIZED TOV MODEL FREE PARAMETERS

In this section we study the behavior of each free parameter of this model on the boundaries of NSs ( $r \rightarrow 0$  and  $r \rightarrow R$ ). Requirements of physically acceptable interior solution for anisotropic static fluid spheres in GR [24–26] can constrain these parameters. This analysis aims to obtain the ranges of the free parameters in the GTOV model since the information from existing observations is insufficient. Furthermore, we should be careful when comparing the GTOV model with ETGs as the TOV equations of each model might not always be the same.

Five conditions should be met if we want the interior solution of fluid spheres to be able accepted physically [24–26]:

- (1) Inside the star,  $\epsilon \geq 0$  and  $P \geq 0$ .
- (2)  $\frac{d\epsilon}{dr} \leq 0$ ,  $\frac{dP}{dr} \leq 0$ , and  $\frac{dQ}{dr} \leq 0$ .
- (3) The speed of sound should be less than the speed of light inside the star.
- (4) The component of the energy-momentum tensor has to obey  $\epsilon + P + 2Q \geq 0$  and  $\epsilon \geq P + 2Q$ .
- (5)  $P = Q$  at the center of the star, but  $P \neq Q$  at the surface since  $P = 0$  but  $Q$  may not vanish.

Note that  $P$  and  $Q$  are the radial and tangential pressure, respectively.

In a realistic and physical description of the interior of stable stars, it is assumed that the spacetime does not possess a singularity. Therefore, the pressure and energy density in the center should be positive and definite. The energy density and pressure should decrease monotonically up to the surface, and become zero at the surface of the stars. Conditions 1 and 2 represent these requirements. If these conditions are satisfied, then the null energy condition, weak energy condition, and strong energy condition (SEC) are also satisfied. Note that the energy conditions are the criteria for a physically admissible energy-momentum tensor in GR. Therefore, the energy conditions are used to rule out nonphysical solutions of the Einstein field equations. The energy density should have a positive value and gravity should encode attractively in these requirements [33]. Condition 3 is the causality condition, i.e., the speed of sound should be subluminal. Condition 4 is an SEC and a trace energy condition (TEC). The TEC is stronger than

the dominant energy condition, i.e.,  $\epsilon \geq P$  and  $\epsilon \geq Q$ . Note that if the TEC holds, anisotropic stars have a larger redshift bound than that of isotropic stars [34]. Condition 5 is related to the behavior of the anisotropic factor at boundaries. In the center, the pressures are at a maximum and tend to be isotropic due to stability reasons, where  $P = Q$  at the center. Meanwhile, the consequences of  $P = 0$  and  $Q \neq 0$  at the surface are the stars (i) more stable [35], (ii) have a relatively massive configuration [35], and (iii) have hard outer mantles [36].

Before we analyze the energy conditions at the center and surface of a NS, we determine the range of  $\sigma$  from condition 4. Note that  $\sigma \equiv P - Q$  so that condition 4 yields two inequalities, i.e.,  $\epsilon - 3P + 2\sigma \geq 0$  and  $\epsilon + 3P - 2\sigma \geq 0$ . Therefore, we conclude that the range of  $\sigma$  can be expressed as

$$-\frac{1}{2}(\epsilon - 3P) \leq \sigma \leq \frac{1}{2}(\epsilon + 3P). \quad (31)$$

Equation (31) is the constraint of  $\sigma$  that obtain from energy conditions. Moreover, this constraint is valid for every model with an effective anisotropic pressure and energy density.

First, we analyze the implications of the energy conditions for the region near the NS center  $r_c$ . The energy density, radial pressure, tangential pressure, anisotropic factor, and NS mass near the NS center are written as  $\epsilon_c = \epsilon(r_c)$ ,  $P_c = P(r_c)$ ,  $Q_c = Q(r_c)$ ,  $\sigma_c = \sigma(r_c)$ , and  $M_c = M(r_c)$ , respectively. Note that  $r_c \rightarrow 0$  and  $M_c \rightarrow 0$ . Based on condition 3,  $(\frac{\epsilon_c}{P_c})_{\max} = 1$ . Based on condition 4,  $(\frac{\epsilon_c}{P_c})_{\min} = 3$ . Note that  $\sigma_c \rightarrow 0$ . Therefore, we obtain a range for the ratio of the energy density and radial pressure,

$$\frac{1}{3} \leq \Upsilon_c \leq 1, \quad (32)$$

where  $\Upsilon_c = \frac{P_c}{\epsilon_c}$ . Note that  $\Upsilon_c$  is insensitive to the details of the NS EOS [37]. Saes and Mendes [37] obtained  $\Upsilon_{\min} \approx 0.300$  using the universal relation between  $\Upsilon_{\min}$  and the compactness  $C$ . In addition, they obtained  $\Upsilon_{\min} = 0.200_{-0.05}^{+0.05}$  from GW170817 which is from the median of 90% credible interval  $\Upsilon$  probability distribution function for primary component and obtained from combination data of NICER and XMM Newton [37]. Therefore, the  $\Upsilon_{\min} = 1/3$  that we obtained from the energy conditions is compatible with those obtained in Ref. [37]. Next, we apply the energy conditions for the anisotropic TOV equations for our case where  $\epsilon \rightarrow \bar{\epsilon}$ . The energy density for the anisotropic TOV equations in our case can be expressed as

$$\bar{\epsilon} = \epsilon + \theta P + \frac{\Gamma\sqrt{\epsilon}M}{4\pi r^2}. \quad (33)$$

Equation (33) is a combination of Eqs. (8) and (10). At the NS center, the third term vanishes since  $M_c \approx \frac{4}{3}\pi r_c^3 \epsilon_c$  and  $r_c \rightarrow 0$ . By applying condition 4, we obtain  $\Upsilon_c \leq \frac{1}{3-\theta}$ . As a consequence of Eq. (32), we obtain a physically acceptable range for the  $\theta$  parameter, i.e.,  $0 \leq \theta \leq 2$ . We need to note that we obtain  $\theta$  equal to zero as the minimum range result since we use  $\Upsilon_{\min} = 1/3$ . Therefore, the range of  $\theta$  is uncertain because of the dependency on the uncertainty of  $\Upsilon_{\min}$ . For instance, if we assume that  $\Upsilon_{\min} < 1/3$ , then we obtain a negative value for  $\theta_{\min}$ , and if we take  $\Upsilon_{\min} \equiv 0.25$ , then we obtain  $\theta_{\min} = -1$ .

Next, we rewrite Eq. (9) in a different form, i.e.,

$$\sigma = \sigma_1 + \sigma_2 \Delta, \quad (34)$$

$$\sigma_1 = -\frac{G\Gamma\sqrt{\epsilon}M(M + 4\pi r^3 P)}{8\pi r^2(r - 2GM)}, \quad (35)$$

$$\sigma_2 = \frac{G(\bar{\epsilon} + P)(M + 4\pi r^3 P)}{2(r - 2GM)}. \quad (36)$$

As a consequence of  $r_c \rightarrow 0$ ,  $\sigma_c \rightarrow 0$ , and  $\sigma_1 \rightarrow 0$  at the NS center,  $\Delta$  has to be zero since  $\sigma_2$  is positive. From  $\Delta = 0$ , we obtain

$$\bar{\alpha} \left( \frac{1}{3} + \left( \chi + \frac{\beta}{3} \right) \Upsilon_c + \beta \chi \Upsilon_c^2 \right) = \frac{1}{3} + \left( 1 + \frac{\bar{\theta}}{3} \right) \Upsilon_c + \bar{\theta} \Upsilon_c^2. \quad (37)$$

Note that  $\bar{\theta} = \theta + 1$ . From Eq. (37), we obtain three equations,

$$\bar{\alpha} = 1, \quad (38)$$

$$\chi + \frac{\beta}{3} = 1 + \frac{\bar{\theta}}{3}, \quad (39)$$

$$\beta \chi = \bar{\theta}. \quad (40)$$

From Eq. (38), we obtain  $\alpha = 0$ . From Eq. (39), we obtain the explicit form of  $\chi$ , i.e.,

$$\chi = \frac{1}{3}(4 + \theta - \beta). \quad (41)$$

By inserting Eq. (41) into Eq. (40), we obtain the quadratic form of  $\beta$ ,

$$\beta^2 - (4 + \theta)\beta + 3(1 + \theta) = 0. \quad (42)$$

If  $\theta = 0$ , we obtain two values for  $\chi$  and  $\beta$ :  $\chi = 1$  with  $\beta = 1$ , and  $\chi = \frac{1}{3}$  with  $\beta = 3$ . If  $\theta = 1$ , we obtain two values for  $\chi$  and  $\beta$ :  $\chi = 1$  with  $\beta = 2$ , and  $\chi = \frac{2}{3}$  with  $\beta = 3$ . If  $\theta = 1$ , we obtain one value for  $\chi$  and  $\beta$ :  $\chi = 1$  with  $\beta = 3$ .

Based on the analysis of energy conditions near the NS center, we obtain the correlated free parameter values of  $\theta$ ,  $\chi$ , and  $\beta$ . Next, we use the energy conditions at the NS surface to obtain estimates of the value of  $\Gamma$ . Before we analyze the energy conditions, we note the following notation for the energy density, radial pressure, tangential pressure, anisotropic factor, and NS mass at the surface ( $r = R$ ):  $\epsilon_R = \epsilon(R)$ ,  $P_R = P(R)$ ,  $Q_R = Q(R)$ ,  $\sigma_R = \sigma(R)$ , and  $M_R = M(R)$ , respectively. From Eq. (18),  $\epsilon_R \rightarrow 0$  since it has to fit the exterior solution with  $\epsilon = 0$  so that  $\bar{\epsilon} \approx 0$  in Eq. (7). From  $\bar{\epsilon} \approx 0$ , we obtain the explicit form of  $\Gamma$ ,

$$\Gamma \approx \frac{4\pi R^2}{M_R} \sqrt{\epsilon_R}. \quad (43)$$

Note that  $\Gamma$  has dimensions  $(\text{fm}/\text{MeV})^{\frac{1}{2}}$ .  $\Gamma \rightarrow 0$  is due to the fact that  $\epsilon_R \rightarrow 0$ . Another argument  $\Gamma \rightarrow 0$  can find from the requirement  $dM/dr \geq 0$  which satisfies evaluating on the surface. To this end, the energy conditions alone can constrain the range of almost all of the GTOV model's free parameters, except for  $\alpha$ . In brief,  $\alpha$  seems to be an independent free parameter in the GTOV model. In the following, we compare the weak-field (nonrelativistic) limit of the GTOV model with some modified gravity theories. We hope that we have insight from other theories about the  $\Gamma$  term and what the range of the  $\alpha$  parameter should be. The nonrelativistic limit of the GTOV model can be expressed as

$$\frac{dP}{dr} = -\frac{GM\epsilon}{r}(1 + \alpha), \quad (44)$$

$$\frac{dM}{dr} = 4\pi r^2 \epsilon \left(1 + \frac{\Gamma\sqrt{\epsilon}M}{4\pi r^2}\right). \quad (45)$$

First, we compare Eqs. (44) and (45) with the general post-Newtonian approach for modified gravity from Ref. [38]. Its equations can be expressed as

$$\frac{dP}{dr} \simeq -\frac{GM\epsilon}{r} - \frac{\kappa_g}{4} \epsilon \frac{d\epsilon}{dr}, \quad (46)$$

$$\frac{dM}{dr} = 4\pi r^2 \epsilon, \quad (47)$$

where  $\kappa_g$  is a free parameter. Note that Eq. (46) neglects terms that violate the equivalence principle in the spherical case [38]. Note that Eqs. (46) and (47) are the same as those predicted by the EiBI theory; see, for example, Refs. [39,40] which discuss EiBI theory in the weak-field limit. Note that the constraint for  $\kappa_g$  depends on the compactness of the objects [4,38–41]. The tightest constrain is NS compactness. This parameter plays a significant role in explaining the hyperon puzzle in NSs; see, for example, the corresponding discussions in Refs. [4,41]. We

can see that  $\alpha \rightarrow 0$  by comparing Eqs. (44) and (46), where  $\kappa_g$  term only appears in EiBI theory and post-Newtonian approach. Therefore, it seems that the role of the  $\alpha$  term in the GTOV model is effectively replaced by the  $\kappa_g$  term in these models. Moreover, we can identify that the  $\Gamma$  term does not appear in the post-Newtonian approach or EiBI theory by comparing Eqs. (45) and (47). Next, we discuss the weak-field limit of the  $f(R)$ -theory-derived result in Ref. [40]. The result is based on the Taylor expansion of  $f(R)$  concerning the Ricci scalar  $R$ , i.e.,  $f(R) \approx C_1 R + C_2 R^2 + \dots$ . Note that  $C_1 \equiv 1 + \delta$  and  $\delta$  is an independent parameter describing the deviation from the GR value of  $C_1$  that may acquire nontrivial values on astronomical scales [40]. For the case of  $C_1 = 1 + \delta$  and  $\zeta = \sqrt{C_1/(6C_2)}$ , the authors of Ref. [40] obtained the gravitation potential  $\Phi$  as

$$\Phi(r) = -\frac{G}{1 + \delta} \int \frac{\rho(\mathbf{r}')}{|\mathbf{r} - \mathbf{r}'|} d^3 r' - \frac{G}{3(1 + \delta)} \int \frac{\rho(\mathbf{r}')}{|\mathbf{r} - \mathbf{r}'|} e^{-\zeta|\mathbf{r} - \mathbf{r}'|} d^3 r'. \quad (48)$$

If we take the long-range limit  $\zeta \rightarrow \infty$  in the second term in Eq. (48), we obtain

$$\frac{dP}{dr} \approx -\frac{GM\epsilon}{r}(1 + \alpha), \quad (49)$$

$$\frac{dM}{dr} = 4\pi r^2 \epsilon, \quad (50)$$

with  $\alpha \approx 1/3 - 4/3\delta$ . Note that if  $\delta \equiv 0$ ,  $\alpha = 1/3$  [22,23,27] and fitting the masses and radii prediction of the model into white-dwarfs data provides the range  $-0.155 < \delta < 0.593$  [40]. In short,  $\alpha$  is not zero, and  $f(R)$  theory does not predict the  $\Gamma$  term. To this end, as shown in Eq. (20), there are indeed ETG models that yield corrections in  $dM/dr$ , e.g., T-squared gravity [31]. However, the corresponding function is different or does not coincide in the weak-field limit with that of  $\Gamma$  term in the GTOV model. Therefore, it is clear from the discussion that  $\alpha$  generally should not equal zero, and extending the PTOV model by adding the  $\Gamma$  term to the GTOV model does not seem too natural.

To this end, we conclude that the value of the GTOV free parameters can be restricted to specific ranges, except for  $\alpha$ . We have found a correlation among  $\theta$ ,  $\chi$ , and  $\beta$ . Moreover, we obtain the parameter  $\Gamma \rightarrow 0$  or the demanding value should be tiny if it is not zero. Besides,  $\alpha$  should not be zero based on the weak-field in some ETGs arguments and observation results.

#### IV. NEUTRON STAR EQUATION OF STATE

In this section we briefly review the NS EOS. We use the usual NS EOS structure, which consists of a crust and a

core. For the NS crust, we use the EOS proposed by Miyatsu *et al.* [42]. For the NS core, we use the relativistic mean field (RMF) model for baryons by including hyperons that can be expressed as [43,44]

$$\mathcal{L} = \mathcal{L}_B + \mathcal{L}_M + \mathcal{L}_L, \quad (51)$$

where  $\mathcal{L}_B$ ,  $\mathcal{L}_M$ , and  $\mathcal{L}_L$  describe baryons, mesons, and leptons, respectively.  $\mathcal{L}_B$  defines as summing of Lagrangian density free baryons and Lagrangian density interaction between through mesons [44], i.e.,

$$\mathcal{L}_B = \sum_B \bar{\Psi}_B \left[ i\gamma^\mu \partial_\mu - (m_B - g_{\sigma B}\sigma) - \left( g_{\omega B}\gamma^\mu \omega_\mu + \frac{1}{2}g_{\rho B}\gamma^\mu \tau_B \cdot \rho_\mu + g_{\phi H}\gamma^\mu \phi_\mu \right) \right] \Psi, \quad (52)$$

where  $m_B$  is the baryon mass. Note that the baryon particles described in Eq. (51) are  $N$ ,  $\Lambda$ ,  $\Sigma$ , and  $\Xi$ . The coupling constants between  $\sigma$ ,  $\omega$ , and  $\rho$  through baryons are denoted by  $g_{\sigma B}$ ,  $g_{\omega B}$ , and  $g_{\rho B}$ , respectively.  $g_{\phi H}$  is the coupling constant between a hidden-strangeness meson and hyperons ( $H = \Lambda, \Sigma$ , and  $\Xi$ ). Note that high-density nuclear matter is a thermodynamic limit of finite nuclei. In this limit,  $B \rightarrow \infty$  and volume  $\rightarrow \infty$ , but the densities are finite. Therefore, in this limit, we have  $\sum_B \rightarrow \int d^3k$ .

$$\mathcal{L}_{\sigma\omega\rho} = \frac{\eta_1 g_{\sigma N} m_\omega^2}{2m_N} \sigma \omega_\mu \omega^\mu + \frac{\eta_2 g_{\sigma N}^2 m_\omega^2}{4m_N^2} \sigma^2 \omega_\mu \omega^\mu + \frac{\eta_\rho g_{\sigma N} m_\rho^2}{2m_N} \sigma \rho_\mu \cdot \rho^\mu + \frac{\eta_{1\rho} g_{\sigma N}^2 m_\rho^2}{4m_N^2} \sigma^2 \rho_\mu \cdot \rho^\mu + \frac{\eta_{2\rho} g_{\omega N}^2 m_\rho^2}{4m_N^2} \omega_\mu \omega^\mu \rho_\mu \cdot \rho^\mu. \quad (59)$$

$\omega^{\mu\nu}$  in Eq. (55) and  $\rho^{\mu\nu}$  in Eq. (56) are  $\omega$  and  $\rho$  meson field tensors, respectively.  $\omega^{\mu\nu}$  and  $\rho^{\mu\nu}$  can be expressed as  $\omega^{\mu\nu} = \partial^\mu \omega^\nu - \partial^\nu \omega^\mu$  and  $\rho^{\mu\nu} = \partial^\mu \rho^\nu - \partial^\nu \rho^\mu$ , respectively. The last term in Eq. (51) describes free leptons (electron and muon) and can be written as

$$\mathcal{L}_L = \sum_L \bar{\psi}_L (i\gamma^\mu \partial_\mu - m_L) \psi_L, \quad (60)$$

where  $m_L$  is the lepton mass. In the present work, we use the BSP parameter set of the RMF model proposed in Ref. [43]. Note that for the nucleon sector, the values of the nucleon coupling constants and nonlinear parameters of the BSP set are tightly constrained by the bulk properties of the finite nuclei and nuclear matter; see Ref. [43] for a detailed optimization procedure to obtain the BSP coupling constants and parameters in the nucleon sectors. Reference [43] also discussed the quality of BSP predictions in finite nuclei and nuclear matter by comparing them with other models and available experimental data. On the contrary, because the hypernuclei are primarily unstable, the coupling constants of hyperons could not be precisely

$\mathcal{L}_M$  is the sum of the Lagrangian densities for the  $\sigma$ ,  $\omega$ ,  $\rho$ ,  $\sigma^*$ , and  $\phi$  mesons and the Lagrangian densities describe cross interactions among  $\sigma$ ,  $\omega$ , and  $\rho$  mesons, which we can write as

$$\mathcal{L}_M = \mathcal{L}_\sigma + \mathcal{L}_\omega + \mathcal{L}_\rho + \mathcal{L}_{\sigma^*} + \mathcal{L}_\phi + \mathcal{L}_{\sigma\omega\rho}, \quad (53)$$

where

$$\mathcal{L}_\sigma = \frac{1}{2} (\partial_\mu \sigma \partial^\mu \sigma - m_\sigma^2 \sigma^2) - \frac{\kappa_3 g_{\sigma N} m_\sigma^2}{6m_N} \sigma^3 - \frac{\kappa_4 g_{\sigma N}^2 m_\sigma^2}{24m_N^2} \sigma^4, \quad (54)$$

$$\mathcal{L}_\omega = -\frac{1}{4} \omega_{\mu\nu} \omega^{\mu\nu} + \frac{1}{2} m_\omega^2 \omega_\mu \omega^\mu + \frac{\zeta_0 g_{\omega N}^2}{24} (\omega_\mu \omega^\mu)^2, \quad (55)$$

$$\mathcal{L}_\rho = -\frac{1}{4} \rho_{\mu\nu} \rho^{\mu\nu} + \frac{1}{2} m_\rho^2 \rho_\mu \rho^\mu, \quad (56)$$

$$\mathcal{L}_{\sigma^*} = \frac{1}{2} (\partial_\mu \sigma^* \partial^\mu \sigma^* - m_{\sigma^*}^2 \sigma^{*2}), \quad (57)$$

$$\mathcal{L}_\phi = -\frac{1}{4} \phi_{\mu\nu} \phi^{\mu\nu} + \frac{1}{2} m_\phi^2 \phi_\mu \phi^\mu, \quad (58)$$

and

constrained. From experimental measurement results, we have only the values of hyperons potential depths at saturation density. Therefore, it is common to use ‘‘prescriptions’’ to determine the hyperon vector coupling constant and employ the potential depths at the nuclear matter saturation density to determine the hyperon scalar coupling constant. The most conservative prescription to determine the hyperon vector coupling constants involves using the SU(6) symmetry of the quark model [45]. Note also that the EOS of NS matter tends to soften when including hyperons. In the case of RMF parameters that are compatible with all terrestrial experimental data like the BSP parameter set, the maximum mass of the NS is less than the NS maximum mass constraint, i.e.,  $\approx 2.1 M_\odot$ . This fact is known as the hyperon puzzle. The possible ways to overcome this issue are as follows. First, one can introduce a phenomenological prescription or use other symmetries like SU(3) to determine the hyperon coupling constants (see Ref. [44] and references therein for details.). Second, one can introduce the possibility that the pressure in NSs can be anisotropic (see Ref. [1] for details related to the interaction between hyperon contributions and anisotropic

contributions confronted with current observational NS data).

Here we use the SU(6) prescription, which is expressed as [45]

$$\begin{aligned}
g_{iN} : g_{i\Lambda} : g_{i\Sigma} : g_{i\Xi} &= 3 : 2 : 2 : 1, \\
g_{jN} : g_{j\Lambda} : g_{j\Sigma} : g_{j\Xi} &= 1 : 0 : 2 : 1, \\
g_{iN} : g_{k\Lambda} : g_{k\Sigma} : g_{k\Xi} &= 3 : \sqrt{2} : \sqrt{2} : 2\sqrt{2}, \quad g_{kN} = 0. \quad (61)
\end{aligned}$$

The potential depth of hyperons can be expressed as [46]

$$U_H^{(N)}(\rho_0) = g_{iH}i(\rho_0) - g_{\sigma H}\sigma(\rho_0). \quad (62)$$

In Eqs. (61) and (62),  $i$ ,  $j$ , and  $k$  denote the  $\omega$ ,  $\rho$ , and  $\phi$  meson, respectively. The experimental values of the potential depth of hyperons at saturation density are given by [45]

$$\begin{aligned}
U_{\Lambda}^{(N)} &= -28 \text{ MeV}, & U_{\Sigma}^{(N)} &= +30 \text{ MeV}, & \text{and} \\
U_{\Xi}^{(N)} &= -18 \text{ MeV}. & & & (63)
\end{aligned}$$

The values in Eq. (63) are used to determine the scalar hyperon coupling constants in the current work. We use an EOS based on this model as input to numerically solve all equations related to NS properties. The results are discussed in the next section.

TABLE I. Parameter sets of the GTOV model to predict NS properties. We vary  $\alpha$  in Sets 1–3.  $0 \leq \theta \leq 2$  appear in Sets 4–7.  $\theta = -1$  appear in Set 8 and Set 9.

Parameter	TOV	Set 1	Set 2	Set 3	Set 4	Set 5	Set 6	Set 7	Set 8	Set 9
$\alpha$	0	0.04	0.095	0.15	0	0	0	0	0	0
$\theta$	0	0	0	0	0	1	1	2	-1	-1
$\beta$	1	1	1	1	3	2	3	3	0	3
$\chi$	1	1	1	1	1/3	1	2/3	1	1	0

TABLE II. Parameter sets of the GTOV model to match with the NS mass-radius from NICER. The set numbers denote that, e.g., in Set 14 the  $\alpha$  value is taken from Set 1 and the other parameters are taken from Set 4 in Table I.

Parameter	TOV	Set 14	Set 15	Set 16	Set 17	Set 18	Set 19
$\alpha$	0	0.04	0.04	0.04	0.04	0.04	0.04
$\theta$	0	0	1	1	2	-1	-1
$\beta$	1	3	2	3	3	0	3
$\chi$	1	1/3	1	2/3	1	1	0

Parameter	TOV	Set 18	Set 28	Set 38	Set 19	Set 29	Set 39
$\alpha$	0	0.04	0.095	0.15	0.04	0.095	0.15
$\theta$	0	-1	-1	-1	-1	-1	-1
$\beta$	1	0	0	0	3	3	3
$\chi$	1	1	1	1	0	0	0

## V. NUMERICAL RESULTS

By obtaining the parameter value range of GTOV from analysis in Sec. III, we make several parameter sets shown in Tables I and II. Those are used to study the physical impact on NS properties. In Table I we provide parameter sets to check the role of each parameter. In this work we set  $\Gamma = 0$ , and we use  $\alpha = 0.04$  in Set 1,  $\alpha = 0.095$  in Set 2, and  $\alpha = 0.15$  in Set 3 to predict the impact of  $\alpha$  on NS properties.  $\alpha$  values are the lowest, middle, and highest values taken from observational cosmology [29]. To predict NS properties, we provide  $\theta$  variation in Sets 4–9. However, we use  $\theta = -1$  (Sets 8 and 9) as a representative

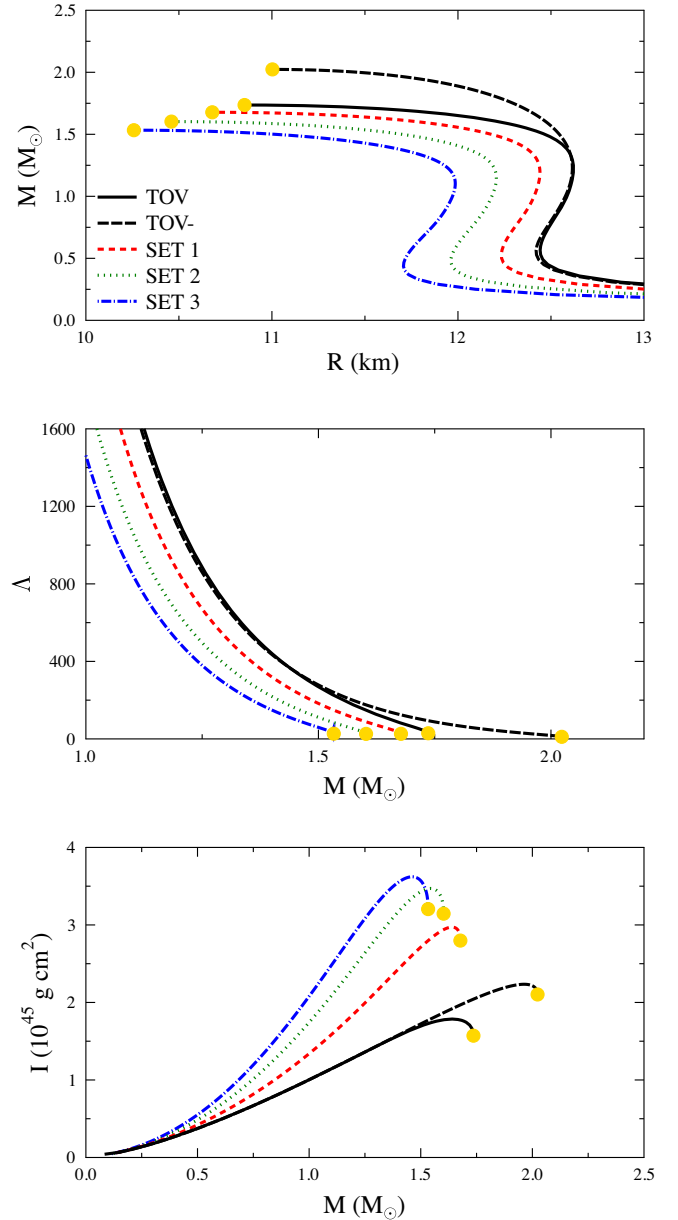


FIG. 1. Impact of  $\alpha$  on NS properties. The gold circle indicates the maximum NS mass.

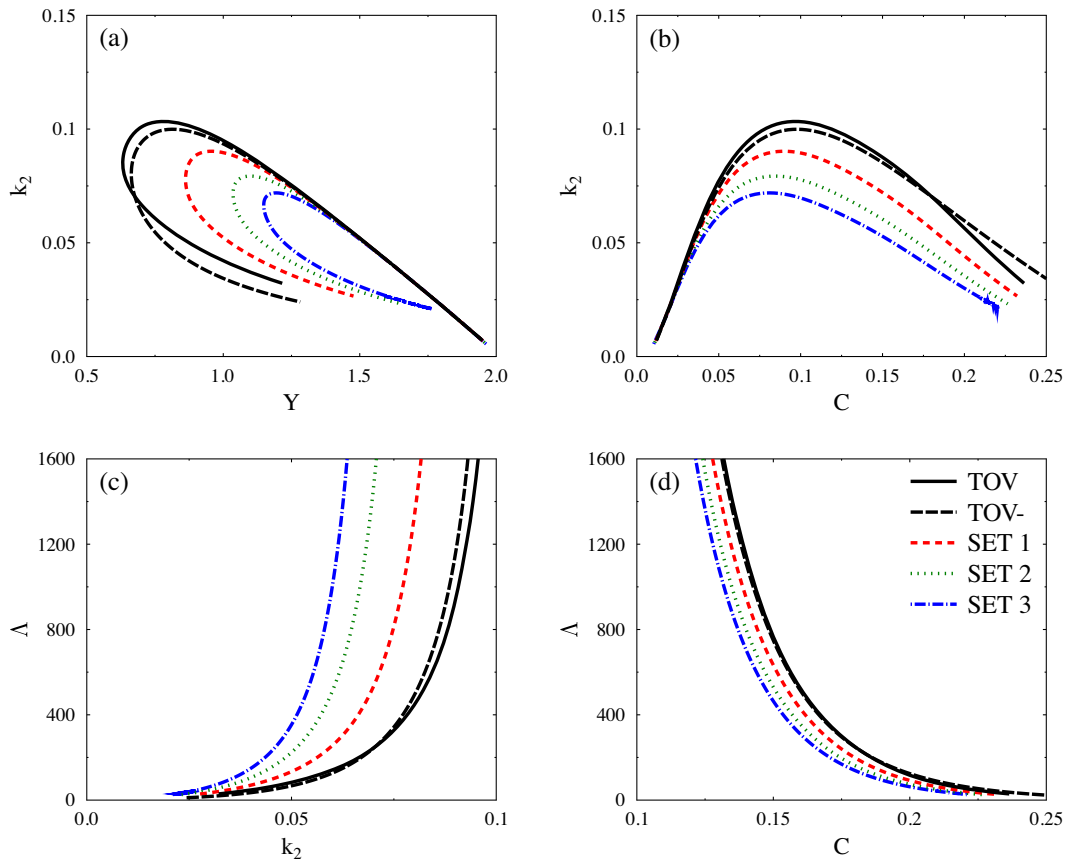


FIG. 2. Impact of  $\alpha$  on  $k_2$  as a function of (a)  $Y$  and (b) the NS compactness and on  $\Lambda$  as a function of (c)  $k_2$  and (d) the NS compactness.

negative value of  $\theta$  since this value cannot be obtained using  $\Upsilon_{\min} = 0.25$  instead of the  $\Upsilon_{\min} = 1/3$  constraint. In Table II we provide combinations of parameter sets from Table I. For example, Set 14 is generated using the  $\alpha$  value taken from Set 1 and the other parameters taken from Set 4 in Table I. We hope that we can gain intriguing impacts on NS properties from parameter value combinations. Note that the moment of inertia provides the information that can connects the mass and radius simultaneously. At the same time, the tidal deformation gives information that cannot be obtained only from the mass-radius relation. Furthermore, in this paper we use mass and radii values from observations of PSR J0030 + 0451 by NICER in 2019 [7,8] and PSR J0740 + 6620 by NICER in 2021 [9,10] as constraints to study whether the GTOV model can solve the hyperon puzzle in NSs. In addition, we also include an EOS without a hyperon—denoted by “TOV-” in all figures—as a comparison with those with hyperons.

The impact of  $\alpha$  on the NS mass-radius relation, moment of inertia, and tidal deformation for Sets 1, 2, and 3 (shown in Table I) is shown in Fig. 1. In the upper and lower panels the  $\alpha$  gives different effect in the maximum mass and the maximum moment of inertia of NS. Increasing  $\alpha$  can decrease the NS maximum mass and increase the NS moment of inertia. Moreover, increasing  $\alpha$  decreases the  $k_2$

peak shown in Figs. 2(a) and 2(b). As a consequence, for the same  $\Lambda$  value, the corresponding mass of NS becomes smaller as shown in the middle panel of Fig. 1. In addition,

TABLE III. Additional information about NS masses around the NS maximum mass calculated using the parameter sets in Table I. Note that  $(R_{\max} + \delta_2)$  is  $R$  of the NS at  $P_c^{\max} + 10$  MeV/fm<sup>3</sup> and  $(R_{\max} - \delta_1)$  is  $R$  of the NS at  $P_c^{\max} - 10$  MeV/fm<sup>3</sup>.  $P_c^{\max}$  is the central pressure for an NS with maximum mass. If  $M(R_{\max} - \delta_1) - M_{\max}$  or  $M(R_{\max} + \delta_2) - M_{\max}$  equal negative, then the maximum masses denoted in figures with gold dot are maximum.

Set	$M(R_{\max} - \delta_1) - M_{\max}$	$M(R_{\max} + \delta_2) - M_{\max}$
TOV	-0.0000747604440421 $M_{\odot}$	-0.0000597884926483 $M_{\odot}$
TOV-	-0.0000672213564741 $M_{\odot}$	-0.0000551032519338 $M_{\odot}$
1	-0.0000533302831444 $M_{\odot}$	-0.0000604642910033 $M_{\odot}$
2	-0.0000439587583361 $M_{\odot}$	-0.0000495651891945 $M_{\odot}$
3	-0.0000425436319525 $M_{\odot}$	-0.0000349895611307 $M_{\odot}$
4	-0.0000908223788454 $M_{\odot}$	-0.0000857824257028 $M_{\odot}$
5	-0.0001122472364268 $M_{\odot}$	-0.0000991124073156 $M_{\odot}$
6	-0.0001279402468302 $M_{\odot}$	-0.0001189420703389 $M_{\odot}$
7	-0.0001443066432006 $M_{\odot}$	-0.0001431342905434 $M_{\odot}$
8	-0.0001977167698524 $M_{\odot}$	-0.0002659681841313 $M_{\odot}$
9	-0.0001083279003677 $M_{\odot}$	-0.0001508951420308 $M_{\odot}$

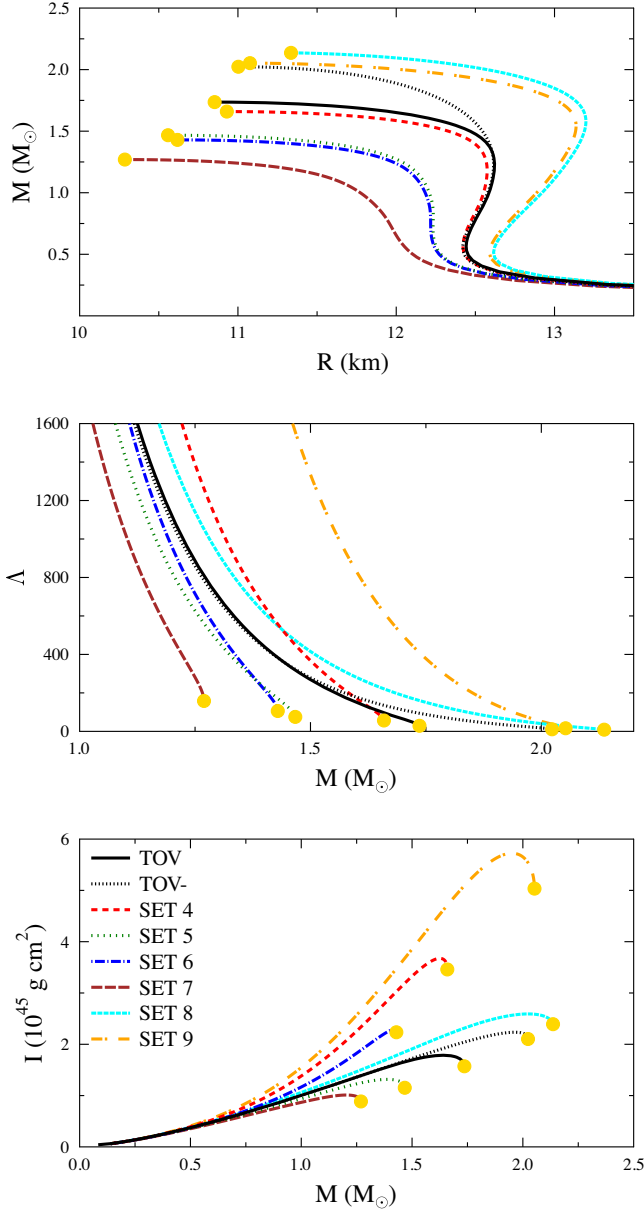


FIG. 3. Impact of the variation of  $\theta$  on NS properties. The gold circle indicates the NS maximum mass.

for the same  $\Lambda$  value,  $k_2$  and compactness significantly increase as shown in Figs. 2(c) and 2(d). Note that to determine the maximum mass denoted by gold dots in all figures, we simply calculate the masses at  $R_{\max} \pm \delta$ , where  $\delta$  is a positive small number with units of meters. If both masses are smaller than the corresponding maximum mass value, then we have the maximum mass value. The results are shown in Table III.

In Fig. 3 we show the impact of the correlated parameters in the GTOV model, i.e.,  $\theta$ ,  $\beta$ , and  $\chi$  on NS properties. As shown in the top panel of Fig. 3, we find that the  $\theta$  value significantly influences the value of NS mass or plays significant role for the maximum mass of NS prediction or

plays the dominant role in predictions of the NS maximum mass. At the same time,  $\beta$  and  $\chi$  can affect predictions of the NS radius and slightly influence the NS mass. These parameters' roles were discussed in Refs. [23,28]. From the NS moment inertia plots in lower panel of Fig. 3, we can check that the  $\beta$  or  $\chi$  parameters impact on NS radius. It is evident from the bottom panel of Fig. 3 that the moment of inertia is quite sensitive to the  $\chi$  value. We can observe that for an NS mass  $M \gtrsim M_{\odot}$ ,  $\chi$  is inversely proportional to the moment of inertia of the NS. Furthermore, from the middle panel of Fig. 3 it is evident that by decreasing the  $\theta$  value, for the same predicted  $\Lambda$  value, the NS mass becomes smaller. However, the pattern of  $\theta$  variation in this plot is not the same as that in the mass-radius relation, shown in the upper panel. The reason of this difference is because  $\beta$  and  $\chi$  parameters also play a role in  $\Lambda$  prediction. The letter can be understood by comparing the  $\Lambda$  results obtained by using Sets 5 and 6. These parameter sets have a similar trend for  $\Lambda$ . However, if we compared the results obtained by using Sets 8 and 9 or the ones obtained by using TOV and Set 4, the  $\Lambda$  results do not show similar behavior. The large difference in  $\Lambda$  results obtained by Sets 8 and 9 or TOV and Set 4 are due to the difference value of  $\beta$  and  $\chi$  parameters. To see the roles of  $\beta$  and  $\chi$  in  $\Lambda$  in more detail, we show the relation of  $\Lambda$  with  $k_2$  and the compactness in Fig. 4. It is evident from Figs. 4(c) and 4(d) that  $\Lambda$  as a function of either  $k_2$  or  $C$  is shifted to the right as  $\chi$  decreases.  $\chi$  also influences the  $k_2$  peak shown in Figs. 4(a) and 4(b). A smaller  $\chi$  predicts a higher  $k_2$  peak. In Fig. 2(a) we can see that Set 9 with  $\chi = 0$  and Set 4 with  $\chi = 1/3$  have a  $k_2$  peak with a negative  $Y$  value, while the rest of the parameter sets (Sets 5–8 and TOV) have a  $k_2$  peak with a positive  $Y$  value. The  $k_2$  peak with a negative  $Y$  value is evidence for an unphysical NS since the  $\chi$  value of Sets 9 and 4 is incompatible with BBN data fitting results [30]. In Fig. 4(a) the highest  $k_2$  value for Set 4 near  $Y = 0$  is  $k_2 \approx 0.166$  ( $Y \approx 0.004$ ). Thus, we use  $k_2 \approx 0.167$  [shown as the magenta line in Fig. 4(b)]. This  $k_2$  value could be considered as the threshold value in order the NS tidal is still physical. Aside from that, we cannot observe a regular trend for the variation of  $\beta$  in  $\Lambda$ . Therefore, we conclude that  $\chi$  plays a more crucial role than  $\beta$  in the tidal deformability predictions of the GTOV model.

After discussing each parameter's impact on NS properties shown in Figs. 1 and 3, we now investigate the impact of the parameter sets collected in Table II on NS properties. The aim is to test whether the GTOV model can solve the hyperon puzzle in NSs. Here we compare the predictions of the corresponding parameter sets with the most recent masses and radii from NS observations. We compare the masses and radii predictions of the parameter sets in Table II with those from observations of PSR J0030 + 0451 by NICER in 2019 [7,8] and PSR J0740 + 6620 by NICER in 2021 [8,10]. It can be seen clearly from Fig. 5 that comparing to the values of  $\alpha$ ,  $\beta$ , and  $\chi$  parameters, the

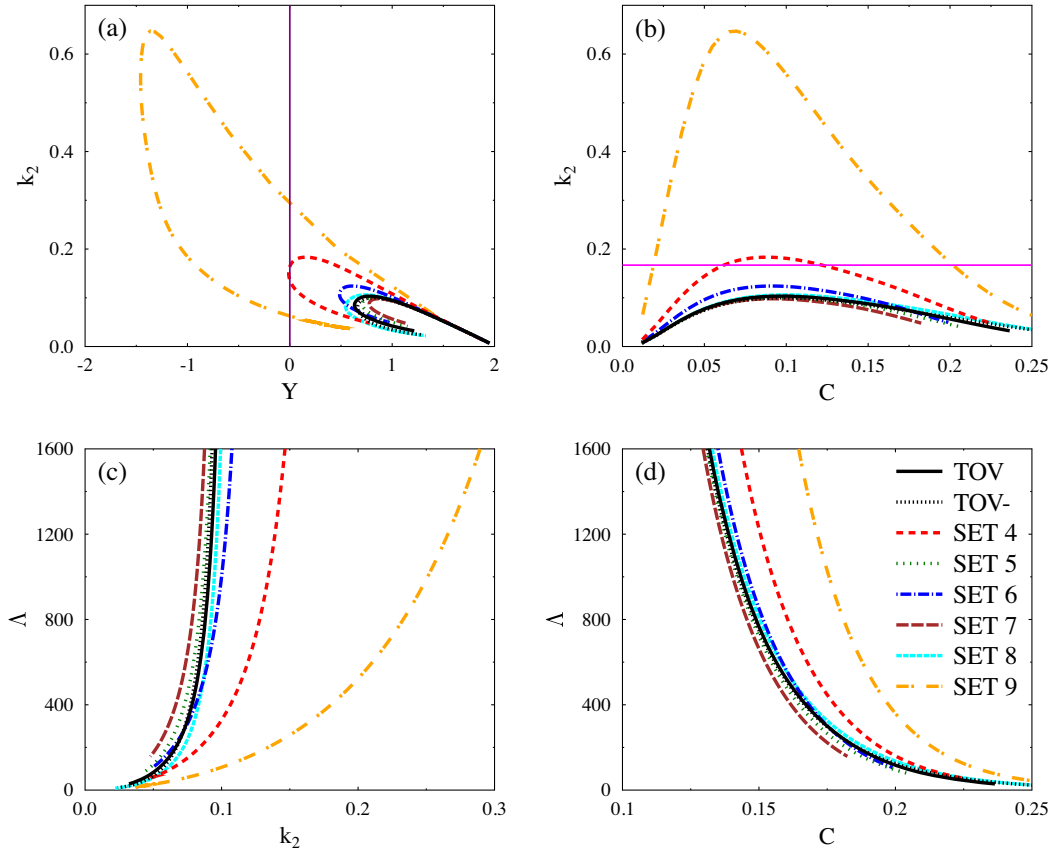


FIG. 4. Impact of the variation of  $\theta$  on  $k_2$  as a function of (a)  $Y$  and (b) the NS compactness and on  $\Lambda$  as a function of (c)  $k_2$  and (d) the NS compactness.

value of  $\theta$  plays more dominant role for controlling maximum mass prediction. In short,  $\theta$  determines the compatibility with the mass and radius observational data of NICER shown in Fig. 5. It can be observed in Fig. 5(a) that the parameter sets with  $-1 \leq \theta \leq 0$  can satisfy constraints from PSR J0030 + 0451 [7,8] and the canonical mass constraint from PSR J0740 + 6620 [9]. Meanwhile, in Fig. 5(b) we can see that all parameter sets can satisfy both constraints, i.e., from both PSR J0030 + 0451 [7,8] and PSR J0740 + 6620 [9]. However, the compatibility of the calculational result with observations can accomplish by using  $\theta = -1$  in these parameter sets. This  $\theta$  value was obtained by using the  $\Upsilon_{\min} = 0.25$  constraint.

To this end, we need to highlight our findings in this study related to the physical meaning of each parameter in the GTOV model.

- (1)  $\alpha$ , which parametrizes the effective gravitational coupling, has a constraint from cosmology [29]. Some modified gravity theories also predict this correction. The simple form of the correction could be seen easily in the corresponding nonrelativistic limit. The results from modified gravity theories seem to produce mainly a density-dependent form for  $\alpha$ , even in the nonrelativistic limit. The properties of NSs are sensitive to the value of this parameter.

For example, by increasing  $\alpha$ , the mass and radius decrease, the moment of inertia increases, and the tidal deformation decreases.

- (2)  $\chi$  is the self-gravity parameter. This parameter is crucial in cosmology and BBN [28,30]. Recently it is reported in Ref. [28] that the NS mass-radius relation cannot be used as a test bed for examining the self-gravity of pressure through  $\chi$  parameter variation from 0 to 1 [28].  $\Lambda$  and  $I$  are sensitive to variations in  $\chi$ .
- (3)  $\beta$  (inertial pressure parameter) and  $\theta$  (gravitational mass parameter) are not independent parameters, as their values are correlated with each other and with  $\chi$  through physically acceptable conditions of the interior solution of fluid spheres. Furthermore, these conditions demand that  $\Gamma$  be zero.
- (4)  $\theta$  plays the most significant role in reproducing the pulsar mass-radius constraints from NICER [7–10].
- (5) It is also evident that the moment of inertia is quite sensitive to  $\beta$ .

The GTOV model has many relative parameters. It is also evident that we have only a few constraints. Therefore, for a quantitative study, a Bayesian statistical analysis to determine the parameter values is admittedly crucial. However, these computations could be rather complex

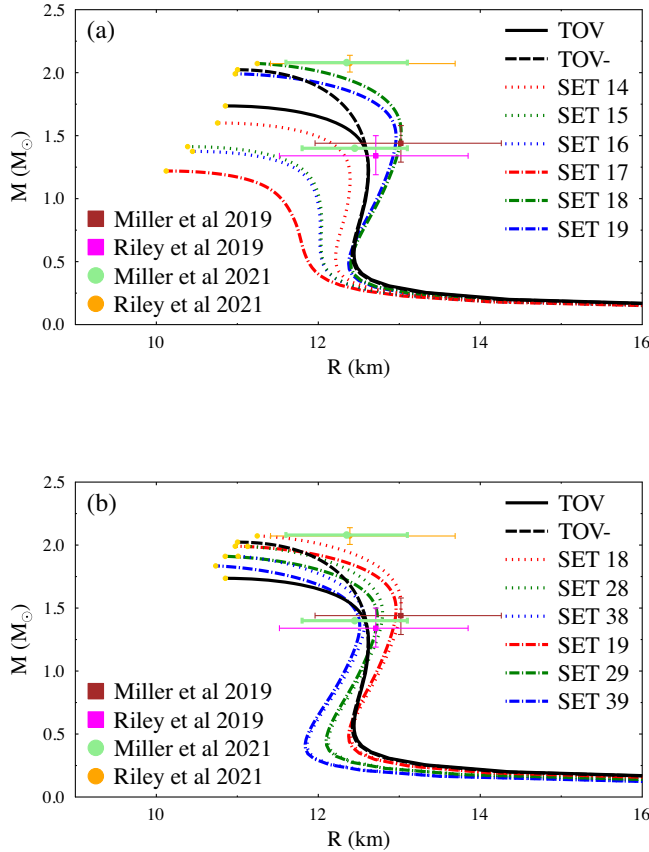


FIG. 5. Impact of the GTOV model parameter sets in Table II on the NS mass-radius relation. Panel (a) shows  $\theta$  varying with  $\alpha$  fixed, i.e.,  $\alpha = 0.04$ . Panel (b) shows  $\alpha$  varying with  $\theta$  fixed, i.e.,  $\theta = -1$ . The gold circle indicates the NS maximum mass. We include constraints from PSR J0030 + 0451 [7,8] and PSR J0740 + 6620 [9,10].

and are already beyond the scope of the present work, so we leave this investigation for our next project.

## VI. CONCLUSIONS

In this work we constructed a modified anisotropic energy-momentum tensor as a standard isotropic energy-momentum tensor by adding a “geometrical correction” to precisely reproduce the TOV equations predicted by GTOV

or PTOV models. The motivation for performing this construction is that we can solve the Einstein field equations using this modified anisotropic energy-momentum tensor to calculate  $I$  and  $\Lambda$ . By obtaining  $I$  and  $\Lambda$ , we were able to explore the role of all free parameters of the GTOV model since we could not obtain sufficient information by only exploring the NS mass-radius relation. For example,  $\chi$  in the GTOV model is a self-gravity of pressure term. The  $\chi$  term is crucial for specific cases, such as cosmology and BBN [28,30]. The authors of Ref. [28] reported that the NS mass-radius relation is not a helpful test bed for examining the self-gravity of pressure through  $\chi$  parameter variation from 0 to 1 [28]. Here we found that  $\Lambda$  is sensitive to variations in  $\chi$ . We also found that the threshold  $k_2$  peak for NSs is  $k_2 \approx 0.167$ . Furthermore, we employed physically acceptable stability conditions for anisotropic objects [24–26] to constrain the GTOV model in the physical range of each parameter value and to investigate the existence of a correlation among the parameters. We found that the value of the GTOV model’s free parameters can be limited to specific physically acceptable ranges except for  $\alpha$ , and it is evident that not all parameters are independent. We found correlations between  $\theta$ ,  $\chi$ , and  $\beta$ . We also found from energy conditions that  $\Gamma$  should be zero, while from the weak field of some selected ETG cases and observational results it is clear that  $\alpha$  should not be zero. With these free parameter ranges in hand, we studied the role of each parameter of the GTOV model in NS properties, including  $I$  and  $\Lambda$ . We also revisited the hyperon puzzle in NSs to test whether the GTOV model with free parameters restriction by energy conditions could resolved this problem. We found that the crucial role of  $\theta$  is to control the NS maximum mass. If we use parameter sets with  $\theta = -1$ , the mass-radius predictions are compatible with recent NICER data [7–10] on PSR J0030 + 0451 and PSR J0740 + 6620. However, this  $\theta$  value does not satisfy the strict  $\Upsilon_{\min} = 1/3$  constraint. Note that the existence of similar form to the  $\theta$  term of GTOV model also predicts by T-squared gravity theory [31]. It is also worth noting that a similar mapping occurs in the case of Rastall-rainbow gravity theory with anisotropic matter, i.e., we can map this gravity theory into GR with a modified anisotropic energy-momentum tensor [47].

- [1] A. Rahmansyah, A. Sulaksono, A. B. Wahidin, and A. M. Setiawan, *Eur. Phys. J. C* **80**, 769 (2020); A. Rahmansyah and A. Sulaksono, *Phys. Rev. C* **104**, 065805 (2021).
- [2] H. Tan, T. Dore, V. Dexheimer, J. Noronha-Hostler, and N. Yunes, *Phys. Rev. D* **105**, 023018 (2022).
- [3] H. Sotani and H. Togashi, *Phys. Rev. D* **105**, 063010 (2022).

- [4] I. Prasetyo, H. Maulana, H. S. Ramadhan, and A. Sulaksono, *Phys. Rev. D* **104**, 084029 (2021).
- [5] H. Boumaza, *Phys. Rev. D* **104**, 084098 (2021).
- [6] A. Saffer and K. Yagi, *Phys. Rev. D* **104**, 124052 (2021).
- [7] M. C. Miller *et al.*, *Astrophys. J. Lett.* **887**, L24 (2019).
- [8] T. E. Riley *et al.*, *Astrophys. J. Lett.* **887**, L21 (2019).
- [9] M. C. Miller *et al.*, *Astrophys. J. Lett.* **918**, L28 (2021).

- [10] T. E. Riley *et al.*, *Astrophys. J. Lett.* **918**, L27 (2021).
- [11] B. P. Abbott *et al.*, *Phys. Rev. Lett.* **119**, 161101 (2017).
- [12] B. P. Abbott *et al.*, *Phys. Rev. Lett.* **121**, 161101 (2018).
- [13] B. P. Abbott *et al.*, *Phys. Rev. X* **9**, 011001 (2019).
- [14] B. P. Abbott *et al.*, *Astrophys. J. Lett.* **896**, L44 (2020).
- [15] I. Arcavi *et al.*, *Nature (London)* **551**, 64 (2017).
- [16] D. A. Coulter *et al.*, *Science* **358**, 1556 (2017).
- [17] I. Legred, K. Chatziioannou, R. Essick, and P. Landry, *Phys. Rev. D* **105**, 043016 (2022).
- [18] M. D. Danarianto and A. Sulaksono, *Phys. Rev. D* **100**, 064042 (2019).
- [19] A. Wojnar and H. Velten, *Eur. Phys. J. C* **76**, 697 (2016).
- [20] J. Ovalle, *Phys. Rev. D* **95**, 104019 (2017).
- [21] V. I. Afonso, G. J. Olmo, and D. Rubiera-Garcia, *Phys. Rev. D* **97**, 021503(R) (2018); V. I. Afonso, G. J. Olmo, E. Orazi, and D. Rubiera-Garcia, *Eur. Phys. J. C* **78**, 866 (2018).
- [22] C. E. Mota, G. Grams, and D. P. Menezes, *arXiv:1811.06445*.
- [23] H. Velten, A. M. Oliveira, and A. Wojner, *Proc. Sci. MPC2015* (**2016**) 025 [*arXiv:1601.03000*].
- [24] L. Herrera and N. O. Santos, *Phys. Rep.* **286**, 53 (1997).
- [25] M. K. Mak and T. Harko, *Proc. R. Soc. A* **459**, 393 (2003).
- [26] A. M. Setiawan and A. Sulaksono, *Eur. Phys. J. C* **79**, 755 (2019); *AIP Conf. Proc.* **1862**, 030001 (2017).
- [27] P. Brax, C. van de Bruck, A. C. Davis, and D. J. Shaw, *Phys. Rev. D* **78**, 104021 (2008).
- [28] J. Schwab, S. A. Hughes, and S. Rappaport, *arXiv:0806.0798*.
- [29] A. Narimani, N. Afshordi, and D. Scott, *J. Cosmol. Astropart. Phys.* **08** (2014) 049.
- [30] S. Rappaport, J. Schwab, S. Burles, and G. Steigman, *Phys. Rev. D* **77**, 023515 (2008).
- [31] Ö. Akarsu, J. D. Barrow, S. Cikintoğlu, K. Y. Ekşi, and N. Katirci, *Phys. Rev. D* **97**, 124017 (2018).
- [32] B. Kumar, S. K. Biswal, and S. K. Patra, *Phys. Rev. C* **95**, 015801 (2017).
- [33] H. Maulana and A. Sulaksono, *Phys. Rev. D* **100**, 124014 (2019).
- [34] B. V. Ivanov, *Eur. Phys. J. C* **78**, 332 (2018).
- [35] H. Abreu, H. Hernández, and L. A. Núñez, *Classical Quantum Gravity* **24**, 4631 (2007).
- [36] H. Hernández and L. A. Núñez, *Can. J. Phys.* **82**, 29 (2004).
- [37] J. Saes and R. F. P. Mendes, *Phys. Rev. D* **106**, 043027 (2022).
- [38] J. Casanellas, P. Pani, I. Lopes, and V. Cardoso, *Astrophys. J.* **745**, 15 (2012).
- [39] C. Wibisono and A. Sulaksono, *Int. J. Mod. Phys. D* **27**, 1850051 (2018); A. S. Rosyadi, A. Sulaksono, H. A. Kassim, and N. Yusof, *Eur. Phys. J. C* **79**, 1030 (2019).
- [40] S. Banerjee, S. Shankar, and T. P. Singh, *J. Cosmol. Astropart. Phys.* **10** (2017) 004.
- [41] A. I. Qauli, M. Iqbal, A. Sulaksono, and H. S. Ramadhan, *Phys. Rev. D* **93**, 104056 (2016).
- [42] T. Miyatsu, S. Yammamuro, and K. Nakazaki, *Astrophys. J.* **777**, 4 (2013).
- [43] B. K. Agrawal, A. Sulaksono, and P.-G. Reinhard, *Nucl. Phys.* **A882**, 1 (2012).
- [44] A. Sulaksono and B. K. Agrawal, *Nucl. Phys.* **A895**, 44 (2012).
- [45] J. Schaffner-Bielich and A. Gal, *Phys. Rev. C* **62**, 034311 (2000).
- [46] N. K. Glendenning and S. A. Moszkowski, *Phys. Rev. Lett.* **67**, 2414 (1991).
- [47] C. E. Mota, L. C. N. Santos, and F. M. da Silva, *Classical Quantum Gravity* **39**, 085008 (2022).